ISBN: 978-3-95450-253-0 ISSN: 2673-5571 doi:10.18429/JACoW-HB2023-THBP36

STUDY OF THE PERFORMANCE OF THE CERN PROTON SYNCHROTRON INTERNAL DUMP

T. Pugnat[1,*], D. Domange[2], L. S. Esposito[1], M. Giovannozzi[1], E. Gnacadja[2], C. Hernalsteens[1], A. Huschauer[1], S. Niang[1], R. Tesse[2]
[1] CERN, Geneva, Switzerland
[2] Université libre de Bruxelles, Brussels, Belgium

Abstract

In the framework of the LHC Injector Upgrade project, a new internal dump for the CERN Proton Synchrotron (PS) has been designed, installed, and successfully commissioned. This device is meant to move rapidly into the beam and stop charged particles over several turns to provide protection to the PS hardware against beam-induced damage. The performance of the dump should ensure efficient use throughout the PS energy range, i.e., from injection at 2 GeV (kinetic energy) to flat top at 26 GeV (total energy). In this paper, detailed numerical simulations are presented, carried out with a combination of sophisticated beam dynamics and beam-matter interaction codes, assessing the behaviour of stopped or scattered particles. The results of these numerical simulations are compared with the data collected during the routine operation of the PS and its internal dump.

INTRODUCTION

During the second long shutdown of the CERN accelerator complex (2019-2021), the internal dumps of the PS ring, installed in straight sections (SS) 47 and 48, have been replaced. This was part of the LHC Injector Upgrade (LIU) [1, 2] project. In fact, the increase in beam brightness imposed a redesign and an upgrade of the dumps. Several studies have been carried out to check the thermomechanical properties of the new dump design [3, 4] as well as its ability to shave the beams [5]. In Ref. [5] a simplified model of beam dynamics in the PS ring was studied with the goal of accessing the multiturn effects in the beam-dump interaction.

The goal of this paper is to further develop the approach presented in Ref. [5] by using a beam dynamics code coupled with a code that simulates the beam-matter interaction. This enables considering the distribution of beam losses along the ring circumference, which is a key observable to assess whether additional shielding might be needed to protect the accelerator hardware. The typical parameters used in the simulations are listed in Table 1. Note that the column "LHC" refers to the proton beam used for the physics at the LHC, a high-brightness beam, while the column "SFTPRO" refers to the proton beam for the fixed-target programme at the CERN Super Proton Synchrotron (SPS) ring, a high-intensity beam. The ultimate goal is to compare the results of the simulation with the beam-based measurements [6].

* thomas.pugnat@cern.ch

Table 1: Typical beam and optics parameters used in the simulations for the PS internal dump, which are taken from the specifications [7, 8].

Parameter	Unit	LHC	SFTPRO
E_t	[GeV]	26.4	14
$\epsilon_x^*/\epsilon_y^*$	[mm mrad]	2.3	9/5
Q_x		6.217	6.247
Q_y		6.280	6.298
Q'_x		1.67	3.93
Q'_y		0.44	1.91
σ_δ	[10^{-3}]	0.4	0.1

MODEL OF THE PS RING

The studies presented in this paper require an accurate representation of the beam dynamics and aperture model along the PS ring as well as the beam-matter interactions occurring in the internal dump and the dynamic change of the dump position must be implemented with care.

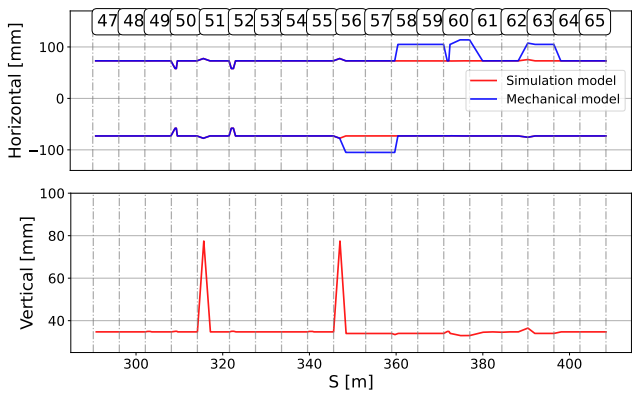

Figure 1: Evolution of the horizontal (top) and vertical (bottom) dimensions of the beam pipe (blue) and of the approximation used in the simulations (red). Note that the vertical aperture is always symmetric around zero and both curves are superposed.

Several chains of simulation codes can be used to achieve the required configuration. `MAD-X` [9], combined with `PTC` [10], is used to generate the optics input for `SixTrack` [11, 12] for which an active coupling [13, 14] with the `FLUKA` code exists [15, 16]. The alternatives consist of using the newly developed tracking code `Xsuite` [17–19], which includes already scattering modules, inherited

ISBN: 978-3-95450-253-0 ISSN: 2673-5571 doi:10.18429/JACoW-HB2023-THBP36

from SixTrack, to deal with the beam-matter interaction, or BDSIM [14, 20–25], which internally uses Geant4 for the beam-matter interaction [26–28]. Comparisons of the three chains, i.e., SixTrack-FLUKA, Xsuite, BDSIM-Geant4, have been carried out and to this extent, the initial conditions for the beam distributions are always generated with Xsuite and are also used with the other codes.

The internal dump has a very complex structure with different materials. Longitudinally, it is divided into two elements: a 12 cm-long graphite block (upstream) and an L-shaped block in copper alloy (CuCr1Zr) with a 10.8 cm thick feet (downstream) [4]. When activated, the dump moves vertically at a speed of 0.8 m/s.

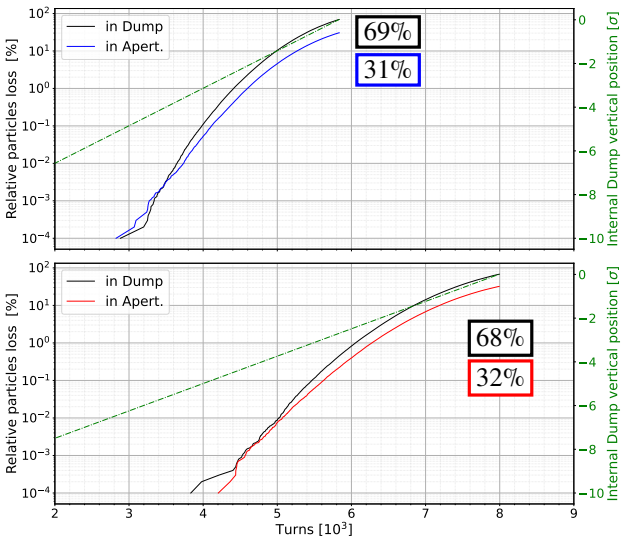

Figure 2: Evolution of the cumulative beam losses as a function of turn for an LHC beam using FLUKA when the dump in SS47 (top) and in SS48 (bottom) are activated. The dashed green line represents the dump position vs turn.

The description of the PS vacuum chamber is an essential aspect of simulations and entails some challenges. The standard vacuum chamber has a cross section close to an ellipse with half axis of 73 mm and 35 mm for horizontal and vertical planes, respectively (note that in reality it is made of four different pieces with two radii). The presence of several extraction regions introduces variations in the cross section of the standard vacuum chamber that is enlarged to provide enough clearance for the extracted beam, including the various extraction bumps. Sometimes the geometrical centre of the cross section is displaced to optimise the beam aperture. The aperture of the beam tube along the circumference of the PS ring is shown in Fig. 1 (blue curves). Clearly visible are some enlargements of the vacuum pipe in the horizontal plane in the region from SS58 to SS63. These features are due to the slow extraction that is performed in the region of the ring. These special cases have still been approximated by an ellipse corresponding to the cross section of a standard beam pipe, but in the future it is planned to model the actual beam pipe cross section using a description by points. In the region between SS47 and SS65, the aperture model (red curve) was refined using the largest ellipse fitting centred on the beam within the actual beam pipe cross section.

NUMERICAL SIMULATIONS

Each simulation consists of computing the evolution of an initial distribution of 10^6 particles (distributed according to the beam parameters listed in Table 1) that are tracked around the ring. Our studies focused on the evolution of cumulative beam losses as a function of turns and their distribution along the accelerator circumference.

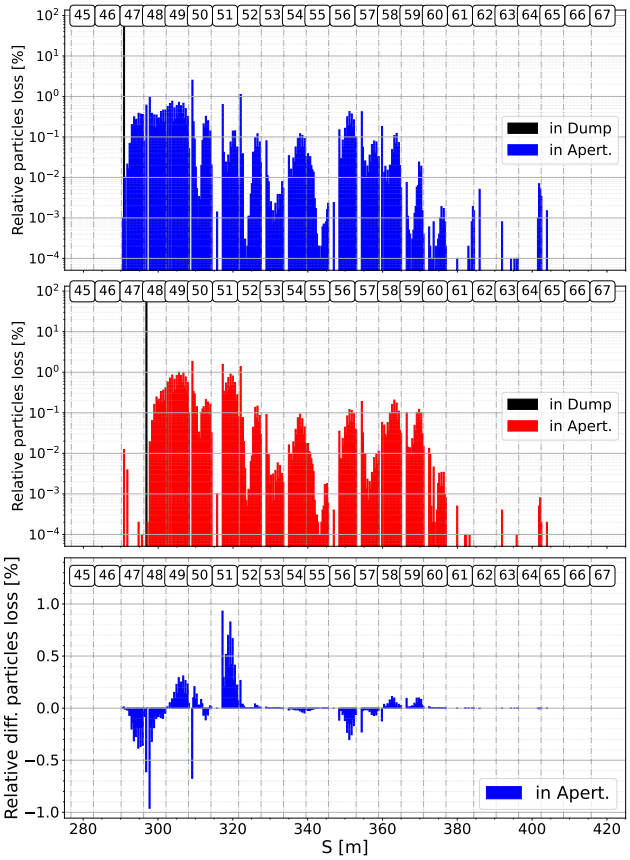

Figure 3: Cumulative distribution of beam losses along the PS ring for an LHC beam using FLUKA when the dump in SS47 (top) and in SS48 (middle) are activated. The difference is also shown (bottom).

The results obtained are shown in Fig. 2 for the LHC case and using FLUKA, and clearly show that a large fraction of the beam impacts the vacuum chamber (approximately 30%) instead of interacting with the internal dump (approximately 70%). Furthermore, it was observed that some particles may survive several turns after their first impact with the dump. The difference in time required to dump the beam is due to the difference in beam size in SS47 and SS48 (note that $\beta_{v,SS47} \approx 11$ m, while $\beta_{v,SS48} \approx 22$ m).

The cumulative distribution of beam losses along the PS circumference is shown in Fig. 3. Losses are restricted to a region of about 120 m downstream of the dump, and the

ISBN: 978-3-95450-253-0 ISSN: 2673-5571 doi:10.18429/JACoW-HB2023-THBP36

difference in the loss distribution generated by the two dumps remains at the percent level of the total number of particles.

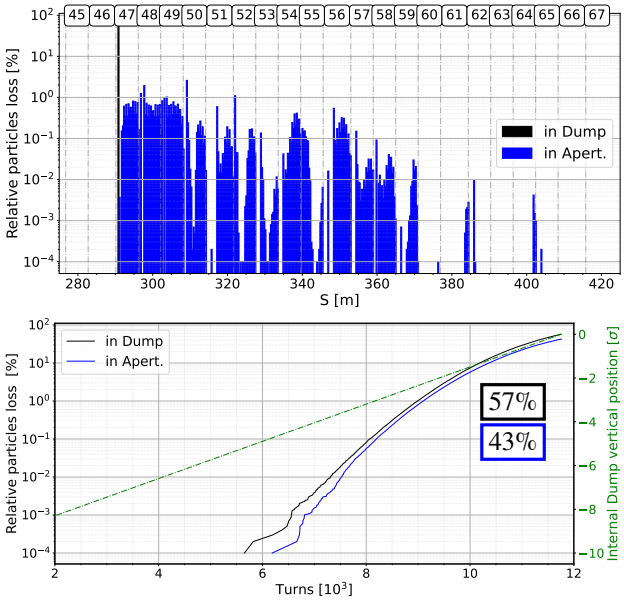

Figure 4: Cumulative distribution of beam losses along the PS ring (top) and evolution of the cumulative beam losses vs turn (bottom) for an SFTPRO beam using FLUKA when the dump in SS47 is activated.

Numerical simulations of the SFTPRO case have also been performed, whose results are shown in Fig. 4. Remarkably, the beam fraction that has a nuclear interaction with the dump is even lower than that for the LHC case, approximately 57 %. Complete beam disposal takes longer, which is mostly a consequence of the larger normalised emittance and lower beam energy of the SFTPRO case relative to LHC. Finally, the extent of the region where beam losses occur is slightly smaller for SFTPRO than for LHC.

Two more aspects have been studied, namely the impact of the longitudinal beam distribution on the beam losses and the comparison between the three chains of codes.

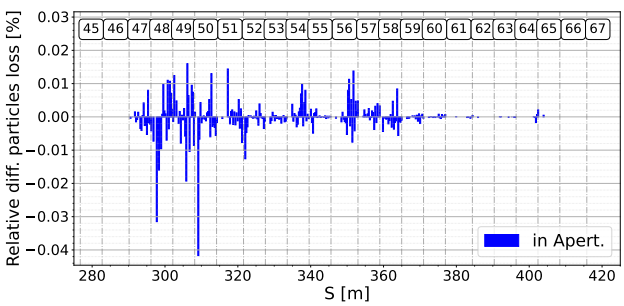

Figure 5: Difference of the beam losses along the PS ring for 6D and 4D tracking simulations for a LHC beam using FLUKA. The differences are essentially negligible.

Tracking simulations have been performed to check whether longitudinal dynamics might be relevant for this study. A distribution has been assigned to the longitudinal coordinates and the RF cavities have been switched on. The comparison between the 4D and 6D simulations is shown in Fig. 5. The small differences can be neglected in practice.

The code comparison is shown in Fig. 6 and due to temporary limitations in the definition of the material in Xsuite, graphite ($\rho = 1.83\,\mathrm{gcm}^{-3}$) is replaced with carbon ($1.67\,\mathrm{gcm}^{-3}$) and CuCr1Zr ($8.9\,\mathrm{gcm}^{-3}$) with Cu ($8.96\,\mathrm{gcm}^{-3}$). Note that not only the beam-matter interaction differs for the various codes, but also the tracking and the algorithm to determine the loss position are not the same. Under these considerations, the overall qualitative agreement is to be considered very good.

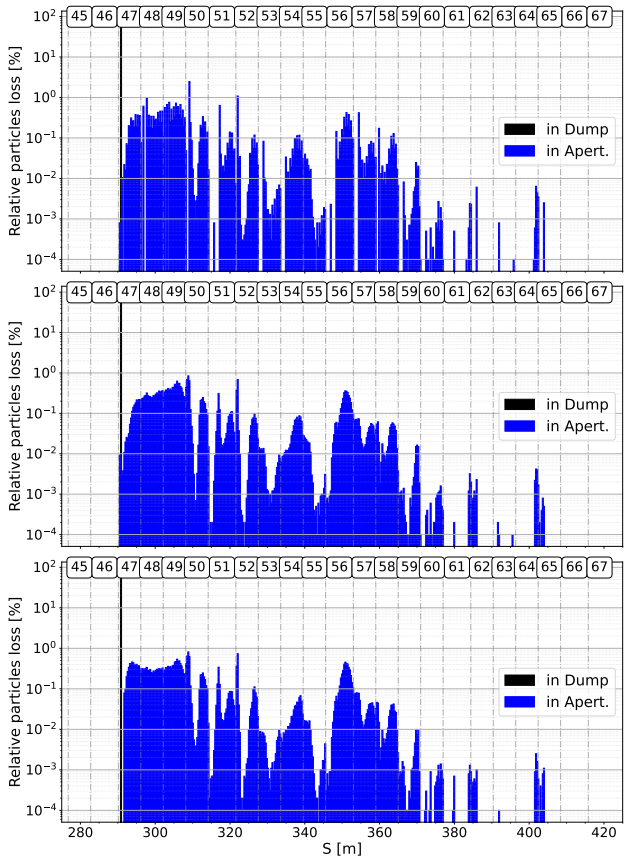

Figure 6: Loss maps in the a LHC beam and dump in SS47 using FLUKA (top), BDSIM (middle) and Xsuite (bottom).

CONCLUSIONS AND OUTLOOK

Detailed beam dynamics simulations of the beam dump process in the PS ring have been carried out and presented in this paper, using three chains of codes.

The results showed that 32 % to 43 % of beam is not stopped by the dump, but impacts the beam pipe over a distance of approximately 1/5 of the ring.

More configurations will be considered to determine the dependence of the losses on beam energy and size and ultimately assess whether the observed beam losses require the implementation of mitigation measures, such as shielding.

ISBN: 978-3-95450-253-0 ISSN: 2673-5571 doi:10.18429/JACoW-HB2023-THBP36

REFERENCES

[1] H. Damerau *et al.*, *LHC Injectors Upgrade, technical design report*. CERN, 2014. doi:10.17181/CERN.7NHR.6HGC

[2] *LHC Injector Upgrade Project*, https://espace.cern.ch/liu-project/default.aspx.

[3] G. Romagnoli *et al.*, "Design of the new PS internal dumps, in the framework of the LHC Injector Upgrade (LIU) Project," in *Proc. IPAC'17*, Copenhagen, Denmark, May 2017, pp. 3521–3523. doi:10.18429/JACoW-IPAC2017-WEPVA109

[4] G. Romagnoli *et al.*, "Engineering design and prototyping of the new LIU PS internal beam dumps," in *Proc. IPAC'18*, Vancouver, Canada, Apr.-May 2018, pp. 2600–2603. doi:10.18429/JACoW-IPAC2018-WEPMG001

[5] J. A. B. Monago *et al.*, "Multi-turn study in FLUKA for the design of CERN-PS internal beam dumps," in *Proc. IPAC'18*, Vancouver, Canada, Apr.-May 2018, pp. 724–727. doi:10.18429/JACoW-IPAC2018-TUPAF025

[6] S. Niang *et al.*, "Shower simulations for the CERN Proton Synchrotron internal dump and comparison with beam loss monitor data," presented at HB'23, Geneva, Switzerland, Oct. 2023, paper THC2C1.

[7] F.-X. Nuiry and G. Romagnoli, "PS ring internal dumps functional specifications," CERN, Tech. Rep., 2017. https://edms.cern.ch/ui/file/1582110/2.1/PS-TDI-ES-0001-20-10.pdf

[8] R. Steerenberg and D. Cotte, "PS Beam spot sizes for the design of new internal beam dumps," CERN, Tech. Rep., 2017. https://edms.cern.ch/ui/file/1612293/1/PS_Beam_Size_Calculations_InternalDumps.pdf

[9] *MAD - Methodical Accelerator Design*, https://mad.web.cern.ch/mad/.

[10] E. Forest, Y. Nogiwa, and F. Schmidt, "The FPP and PTC libraries," in *Proc. 9th Int. Computational Accelerator Physics Conf. (ICAP'06)*, Chamonix, Switzerland, 2006, pp. 17–21. https://jacow.org/icap06/papers/MOM1MP02.pdf

[11] R. De Maria *et al.*, SixTrack – *6D Tracking Code*, http://sixtrack.web.cern.ch/SixTrack/.

[12] R. D. Maria *et al.*, "SixTrack version 5: status and new developments," in *Proc. IPAC'19*, Melbourne, Australia, May 2019, pp. 3200–3203. doi:10.18429/JACoW-IPAC2019-WEPTS043

[13] A. Mereghetti *et al.*, "SixTrack-FLUKA active coupling for the upgrade of the SPS scrapers," in *Proc. IPAC'13*, Shanghai, China, May 2013, pp. 2657–2659. https://jacow.org/IPAC2013/papers/WEPEA064.pdf

[14] *ICFA Mini-Workshop on tracking for collimation in particle accelerators*, CERN, 2018. doi:10.23732/CYRCP-2018-002

[15] C. Ahdida *et al.*, "New capabilities of the FLUKA multi-purpose code," *Front. Phys.*, vol. 9, 2022. doi:10.3389/fphy.2021.788253

[16] G. Battistoni *et al.*, "Overview of the FLUKA code," *Ann. Nucl. Energy*, vol. 82, pp. 10–18, 2015. doi:10.1016/j.anucene.2014.11.007

[17] P. Kicsiny, D. Schulte, G. Iadarola, T. Pieloni, and X. Buffat, "Benchmark and performance of beam-beam interaction models for Xsuite," in *Proc. IPAC'23*, Venice, Italy, 2023, pp. 686–689. doi:10.18429/JACoW-IPAC2023-MOPL063

[18] D. Demetriadou, A. Abramov, G. Iadarola, and F. V. der Veken, "Tools for integrated simulation of collimation processes in Xsuite," in *Proc. IPAC'23*, Venice, Italy, 2023, pp. 2801–2804. doi:10.18429/JACoW-IPAC2023-WEPA066

[19] G. Iadarola *et al.*, "Xsuite: an integrated beam physics simulation framework," presented at HB'23, Geneva, Switzerland, Oct. 2023, paper TUA2I1.

[20] L. J. Nevay *et al.*, "Beam delivery simulation: BDSIM - development & optimisation," in *Proc. IPAC'14*, Dresden, Germany, Jun. 2014, pp. 182–184. doi:10.18429/JACoW-IPAC2014-MOPRO045

[21] L. J. Nevay *et al.*, "Beam Delivery Simulation: BDSIM - automatic Geant4 models of accelerators," in *Proc. IPAC'16*, Busan, Korea, 2016, pp. 3098–3100. doi:10.18429/JACoW-IPAC2016-WEPOY046

[22] L. J. Nevay *et al.*, "Recent developments in beam delivery simulation - BDSIM," in *Proc. IPAC'18*, Vancouver, Canada, Apr.-May 2018, pp. 3266–3269. doi:10.18429/JACoW-IPAC2018-THPAK025

[23] L. J. Nevay *et al.*, "BDSIM: recent developments and new features beyond V1.0," in *Proc. IPAC'19*, Melbourne, Australia, May 2019, pp. 3259–3262. doi:10.18429/JACoW-IPAC2019-WEPTS058

[24] L. J. Nevay *et al.*, "Recent BDSIM related developments and modeling of accelerators," in *Proc. IPAC'21*, Campinas, Brazil, May 2021, pp. 4208–4211. doi:10.18429/JACoW-IPAC2021-THPAB214

[25] L. Nevay *et al.*, "BDSIM v1.7.0 developments for the modelling of accelerators and their environment," in *Proc. IPAC'23*, Venice, Italy, 2023, pp. 2821–2824. doi:10.18429/JACoW-IPAC2023-WEPA074

[26] S. Agostinelli *et al.*, "Geant4—a simulation toolkit," *Nucl. Instrum. Methods Phys. Res., Sect. A*, vol. 506, no. 3, pp. 250–303, 2003. doi:10.1016/S0168-9002(03)01368-8

[27] J. Allison *et al.*, "Geant4 developments and applications," *IEEE Trans. Nucl. Sci.*, vol. 53, no. 1, pp. 270–278, 2006. doi:10.1109/TNS.2006.869826

[28] J. Allison *et al.*, "Recent developments in Geant4," *Nucl. Instrum. Methods Phys. Res., Sect. A*, vol. 835, pp. 186–225, 2016. doi:10.1016/j.nima.2016.06.125